Bull. Mater. Sci., Vol. 34, No. 7, December 2011, pp. 1639–1644. © Indian Academy of Sciences.

Solid-state titania-based gas sensor for liquefied petroleum gas detection at room temperature

B C YADAV*, ANURADHA YADAV, TRIPTI SHUKLA and SATYENDRA SINGH

Nanomaterials and Sensors Research Laboratory, Department of Physics, University of Lucknow, Lucknow 226 007, India

MS received 27 May 2010; revised 21 July 2010

Abstract. This paper reports the liquefied petroleum gas (LPG) sensing of titanium dioxide (Qualigens, India). Scanning electron micrographs and X-ray diffraction studies of samples were done. SEM shows that the material is porous and has grapes-like morphology before exposure to the LPG. XRD patterns reveal the crystalline nature of the material. The crystallites sizes of the TiO_2 were found in the range of 30–75 nm. Variations in resistance with exposure of LPG to the sensing element were observed. The average sensitivity for different volume percentages of gas was estimated. The maximum value of average sensitivity was 1·7 for higher vol.% of LPG. Percentage sensor response (%SR) as a function of time was calculated and its maximum value was 45%. Response time of the sensor was 70 s. The sensor was quite sensitive to LPG and results were found reproducible.

Keywords. LPG sensor; TiO_2; SEM; XRD; sensitivity.

1. Introduction

There is an increasing interest to find new materials in order to develop high-performance solid-state gas sensors. Semiconductor metal oxide sensors are alternative for inexpensive and robust detection systems. Semiconducting metal oxide material such as ZnO, TiO_2, SnO_2, In_2O_3, etc., play an important role in almost all fields of electronics (Yadav *et al* 2008, 2009), especially their applications to gas sensors, which require controlled nanosize of the sensing materials.

TiO_2 is an important oxide material for broad range of gas-sensing applications (Yadav *et al* 2007; More *et al* 2009) because of its surface chemistry, charge transport and electrical properties (Carney *et al* 2005; Manera *et al* 2007). It is a versatile material widely used in industry, research and environmental cleaning. Physical properties of TiO_2 have given various fields of investigation to researchers, which make it suitable for various applications (Lee *et al* 2000; Devi *et al* 2002; Coronado *et al* 2003; Faramarz *et al* 2005; Dhawale *et al* 2008; Thiagarajan *et al* 2009). The first titania gas sensor was developed in the late 1970s and early 1980s, and primarily used to detect the stoichiometric air to fuel ratio (A/F) (Micheli 1984). It was also used to detect a wide variety of gaseous species such as O_2 (Kirner *et al* 1990; Li and Chen 1996), H_2 (Birkefeld *et al* 1992), CO (Bonini *et al* 2000) and NO_x (Guidi *et al* 1999). TiO_2 powder can exist in the anatase, rutile or brookite phase, with the most stable form being rutile, to which the others will convert at sufficiently high temperatures. The brookite phase has an orthorhombic crystal structure, and although similar to rutile in its mechanical properties, it is rarely used commercially. In contrast, the anatase and rutile forms are tetragonal systems that have found wide applications (Wu 2009). Among these, the anatase phase is known to exhibit better gas-sensing behaviour where as rutile is the most stable phase. Even though the energy band gap (3·239 eV) of the anatase phase is wider than that of the rutile (3·02 eV) structure, recombination of electrons and holes occurs much faster on surface of rutile phase. Since the gas-sensing behaviour is mostly confined to the surface of the sensing material, its surface area must be increased to maximize this gas-sensing behaviour (Baruwati *et al* 2006; Shinde *et al* 2007).

2. Experimental

The starting material was TiO_2 (Qualigens, 98% pure) and glass powder. Glass powder was used as binder. These were made fine on grinding in mortar with pestle for 6–8 h. The pelletization of this material having dimensions 9 mm in diameter and 5 mm in thickness was done by using hydraulic press (M.B. Instruments, Delhi, India) under an uniaxial pressure of 462 MPa at room temperature. This pellet was heat-treated in an electric furnace (Ambassador, India) at 400°C for 3 h, and after annealing it was exposed to liquefied petroleum gas (LPG) in

*Author for correspondence (balchandra_yadav@rediffmail.com)

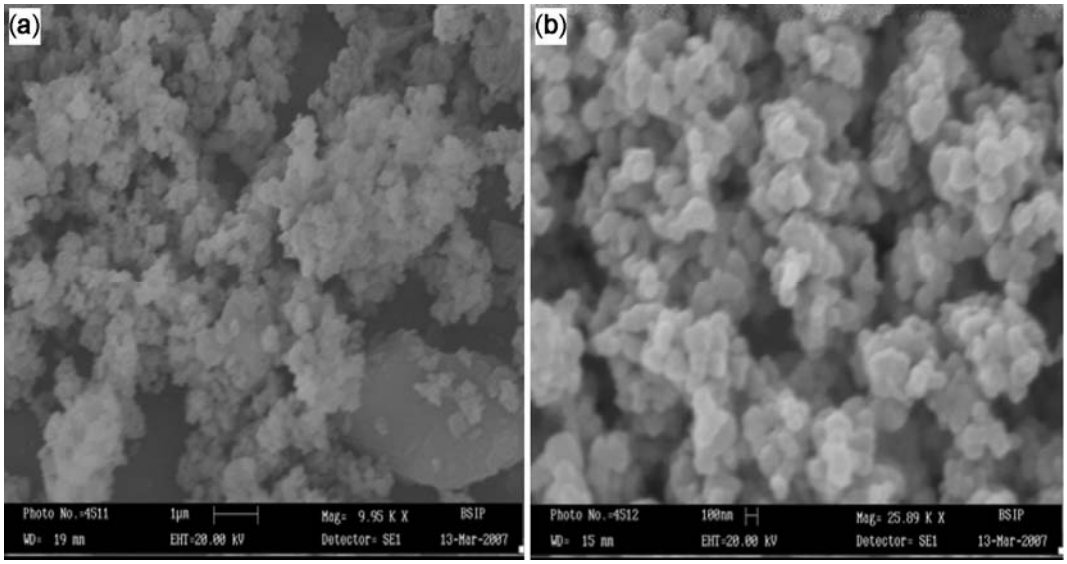

Figure 1. SEM of TiO_2 in form of pellet: (**a**) at microscale and (**b**) at nanoscale.

a specially designed gas chamber in controlled conditions. The corresponding variations in resistance with the time were recorded by using a digital multimeter.

3. Characterizations of synthesized material

3.1 *Surface morphology*

Surface morphology of sensing element was studied using scanning electron microscope unit (SEM, LEO-0430, Cambridge). Scanning electron micrographs of the sensing element annealed at 400°C are shown in figure 1a on microscale and at low magnification (9·95 KX), and figure 1b on nanoscale and at high magnification (25·89 KX). SEM shows that crystallites of TiO_2 combining with adhesive glass particles form beautiful grapes-like clusters, leaving more spaces as pores.

Higher porosity increases the surface-to-volume ratio of the materials, which in turn increases the diffusion rate of gas and therefore helps in getting good sensitivity. SEMs show that the crystallites are agglomerated, uniform in size and equally distributed.

3.2 *X-ray diffraction*

X-Ray diffraction pattern shown in figure 2 obtained by X-Pert, PRO XRD system (Netherland) reveals crystalline nature of the sample. The average crystallite size of the sensing material was calculated by Debye–Scherer formula, which is as follows:

$$D = \frac{K\lambda}{\beta \cos\theta},$$

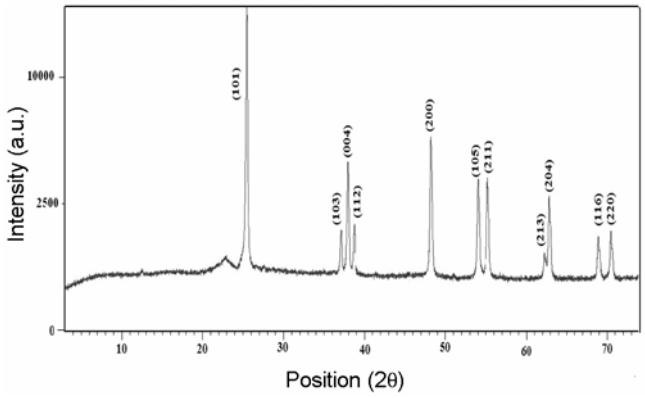

Figure 2. XRD pattern of sensing material in the form of powder.

where D is the average size of crystallite assuming it to be cubic three dimensional, $K = 0{\cdot}94$, λ the wavelength of X-ray radiation having value 1·5418 Å, β the full width at half maximum (FWHM) of the diffraction peak and θ the angle of diffraction.

The XRD pattern shows a high-intensity peak, centered at $2\theta = 25°$, assigned to tetragonal TiO_2 (101) reflection having d spacing 3·5180 Å and FWHM 0·17°. Also, a peak with a low intensity at $2\theta = 70°$ is assigned to TiO_2 (220) reflection having d spacing 1·33473 Å and FWHM 0·4°. The other intense peak is at $2\theta = 38°$ with d spacing and FWHM 2·37997 Å and 0·33°, respectively corresponding to plane (112). Other higher angle of reflections such as (200) and (211) were indicating crystalline nature of TiO_2. The XRD data thus, confirm the formation of TiO_2. The minimum crystallite size of the TiO_2 was 30 nm corresponding to reflection (105) with d

spacing and FWHM 1·70034 Å and 0·315°, respectively, indicating its nanocrystalline behaviour.

4. Gas-sensing characteristic

The pellet of the sensing element is subjected to exposition of LPG. Variations in resistance have been taken with the variation of the time in seconds. The gas sensitivity is defined as

$$S = \frac{R_{\text{air}}}{R_{\text{gas}}},$$

where R_{air} and R_{gas} stand for the resistance of the sensor in air and in the sample gas, respectively (Srivastava *et al* 2006).

Sensor response of a sensing material (Yadav *et al* 2008, 2009) is defined as

$$\%\text{SR} = \frac{|R_{\text{a}} - R_{\text{g}}|}{R_{\text{a}}} \times 100.$$

5. Results and discussion

During experiment, every time, prior to exposing the LPG to TiO_2 pellet, it was allowed to equilibrate inside the gas chamber at room temperature for 20–25 min and the stabilized resistance was taken as R_{a}. The stabilization of the sensing element in ambient air is important because it ensures the stable zero level for gas-sensing applications. The variations in resistance with the exposure time for different vol.% of LPG were observed and are shown in figure 3. Due to *n*-type behaviour of TiO_2, the electrical conductivity increases with reducing gas like LPG, and hence, the resistance of the sensing material decreases with time of exposure to the gas. It is evinced from figure 3 that the sensor resistance decreased rapidly within a few seconds and then increased and further exhibited a stable value. More *et al* 2008 observed similar behaviour for TiO_2 films after annealing at 698 K. The variation of gas sensitivity with time is shown in figure 4. The maximum sensitivity was 1·8 for 5 vol.% of LPG. It has an average gas sensitivity of 1·7 for 5 vol.% of LPG, as shown in

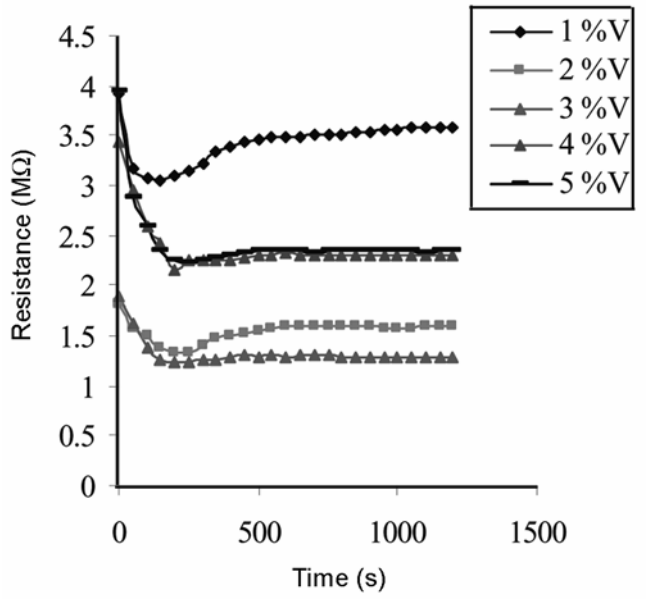

Figure 3. Resistance of sensing material vs time after exposure.

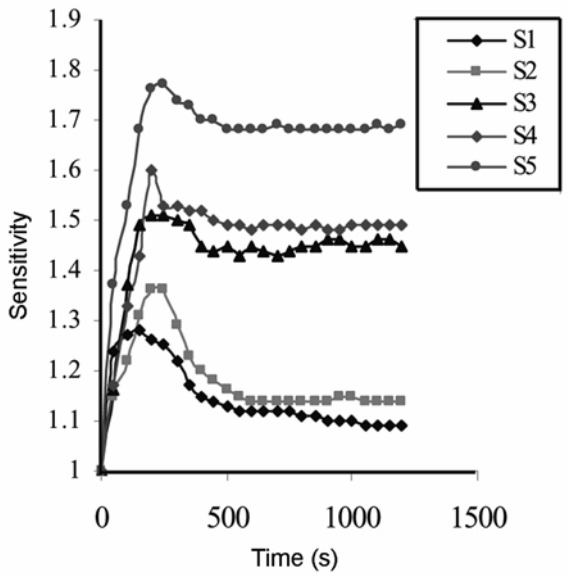

Figure 4. Sensitivity of the sensing material vs time after exposure.

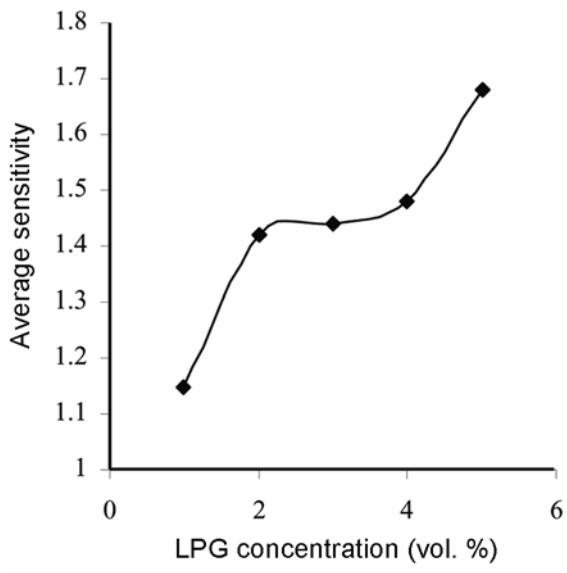

Figure 5. Average sensitivity of sensing material vs concentration of LPG.

figure 5. Gas response curves drawn in figure 6 show that when the LPG was introduced in the gas chamber, the response increased with time during which the gas was exposed. Response time is the time during which the sensor attains 90% of its maximum response. Its value for the sensing element was 70 s. Figure 7 shows the variation of resistance with temperature. At a higher temperature range, as the temperature increases, the resistance of the sensing material decreases. This shows the *n*-type behaviour of the sensing material (Chen *et al* 2008). The Arrhenius plot shown in figure 8 presents the variations of logarithmic resistance as a function of inverse temperature. This establishes the semiconducting nature of the material which is due to the thermally activated mobility of carriers rather than to a thermally activated generation of these. The activation energy determined from the Arrhenius plot was 0·93 eV. Figure 9 shows the reproducibility curve for higher volume, i.e. 5 vol.% of LPG. The sensor is reproducible within ± 95% accuracy. The ageing effect on the sensing material was investigated and is plotted in figure 10. It was observed that the performance of device was affected by ~10% after 3 months.

The principle of operation of the semiconductor gas sensor is based on the interaction of gas molecules with the surface, which produces an interchange or trapping of free charge carriers (Liu *et al* 2008). This sensing

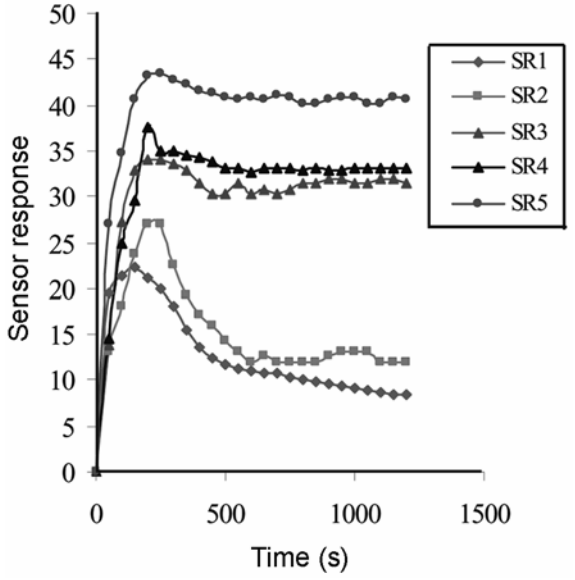

Figure 6. Sensor response vs time after exposure for sensing material.

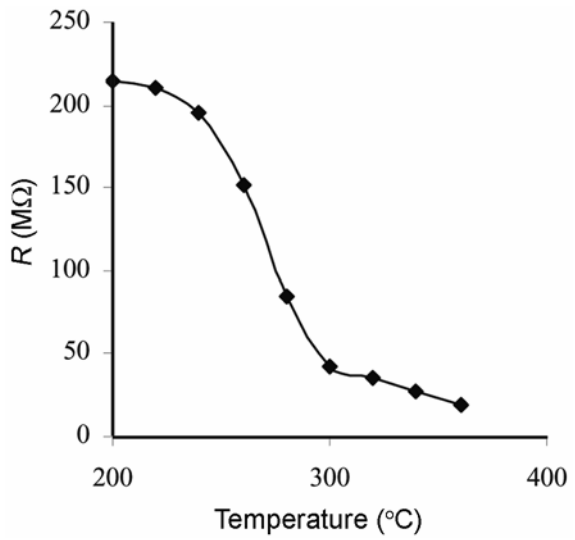

Figure 7. Resistance vs temperature for the sensing element.

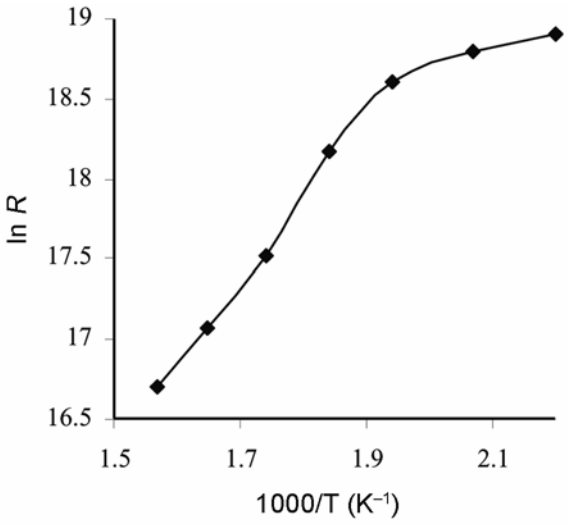

Figure 8. Arrhenius plot for sensing element.

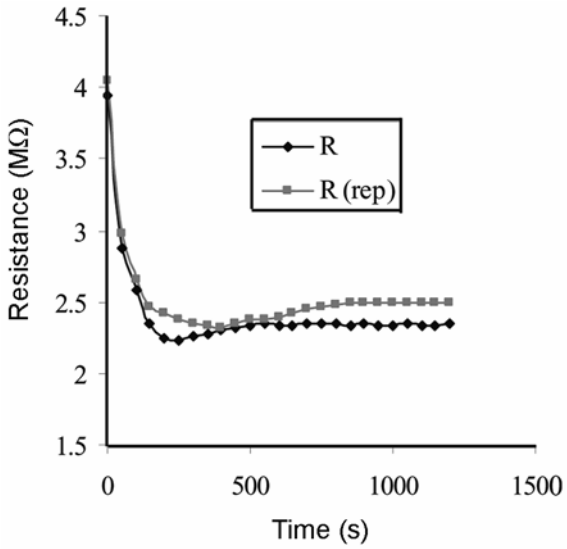

Figure 9. Reproducibility curve for sensing element exposed with 5 vol.% LPG.

mechanism implies that the surface of the material is extremely important from the basic point of view. Three key factors have been recognized to control the sensor response, i.e. the receptor function, the transducer function and the utility factor. The receptor function is supplied either by the surface of the grain or by a foreign material dispersed on them (Cabot *et al* 2000; Ruiz *et al* 2005). The transducer function is related to the grain boundaries and intensified extraordinarily when the grain size becomes smaller than twice the thickness of the space charge layer (Kitamura and Yokoyama 1991; Barsan *et al* 2007). The utility factor is the ratio of the grains accessible for the target gas. Thus, obtaining small particles would improve the sensing efficiency. In the case of TiO_2, these parameters can be effectively controlled by hydrothermal treatment.

The electrical characteristics of TiO_2 critically depend on the chemical composition of the surface and work function. In our experiment, surface sites of the TiO_2 and the electron acceptor properties, the adsorption, the surface reaction and subsequent desorption of the LPG are key factors to determine its performance.

Metal oxide semiconductors are mainly used to detect small concentrations of reducing and combustible gases in air. In the absence of LPG, O_2^- gets adsorbed on the surface of TiO_2 pellet and it extracts electrons from the conduction band creating a depletion layer at the surface of the individual grains and intragranular region. Thus, equilibrium of the chemisorption process results in the stabilization of the surface resistance. When we expose the LPG to the surface area of semiconducting oxide, reaction takes place between surface molecules and LPG. The interaction mechanism between the gas phase and the sensing material involves mainly physiosorption, chemisorption, surface defects and bulk defects.

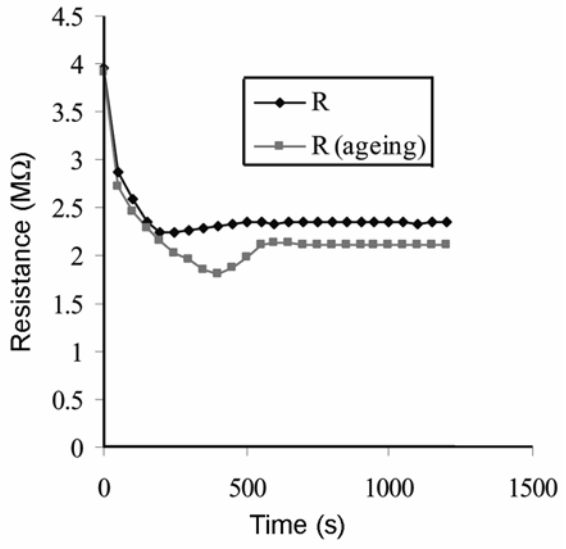

Figure 10. Ageing effect after 3 months for sensing element exposed with 5 vol.% LPG.

Physisorption is the weakest form of adsorption to solid surface and is essentially maintained by the van der Waal interaction. On the other hand, chemisorption is a stronger interaction that shows a better sensitivity and selectivity. In this kind of interactions adsorbate forms chemical bonds with the surface atoms and thus the electronic structure of both the adsorbate and the surface are modified. Chemisorption is usually promoted by surface defects. For these sensors, the defect chemistry of the oxide is very important because the bulk of the material must equilibrate with the oxygen in the system. The change in electrical conductivity of the material has been represented by the following equation

$$\sigma \sim \sigma_0 \exp(E_a/kT) p(O_2)^{1/n},$$

where σ is the electronic conductivity, E_a activation energy, k the Boltzmann constant, T the temperature, $p(O_2)$ the partial pressure of gaseous oxygen and n a value that depends on the nature of the point defects arising when oxygen is removed from the lattice.

The reactions occurring on the surface of TiO_2 gas sensor can be summarized as

$$e^- + O_2 \xrightarrow{T<500K} O_2^-$$

$$e^- + O_2^- \xrightarrow{T>500K} 2O^-$$

$$C_nH_{2n+2} + 2O^- \longleftrightarrow H_2O + C_nH_{2n}O + e^-,$$

where C_nH_{2n+2} represents various hydrocarbons.

The first two reactions takes place in air, due to which carrier concentration is low and thus, increasing the resistance. The last reaction corresponds to oxidation of reducing carriers. This increases the carrier concentration and hence decreases the resistance on exposing to reducing gases.

6. Conclusions

Earlier investigators have not made experimentations for titania at room temperature; they have investigated it at other higher temperatures. Therefore, the research in this paper has demonstrated the possibility and potential of a nanosized TiO_2-based sensor operable at room temperature for sensing of LPG. SEM micrographs show a cluster like morphology with highly porous structure. From XRD, minimum crystallite size was 30 nm. The average sensitivity of sensor was 1·7. Rapid sensor response, good stability and satisfactory sensitivity demonstrate the promise of this sensor for LPG determination in the industrial and environmental monitoring.

Acknowledgements

Financial support from UGC as Major Research Project F. No. 36-265/2008 (SR) is highly acknowledged.

References

Barsan N, Koziej D and Weimar U 2007 *Sensors & Actuators* **B121** 18

Baruwati B, Kumar D K and Manorama S V 2006 *Sensors & Actuators* **B119** 676

Birkefeld L D, Azad A M and Akbar S A 1992 *J. Am. Ceram. Soc.* **75** 2964

Bonini N, Carotta M C, Chiorino A, Guidi V, Malagù C, Martinelli G, Paglialonga L and Sacerdoti M 2000 *Sensors & Actuators* **B68** 274

Cabot A, Arbiol J, Morante J R, Weimar U, Barsan N and Gopal W 2000 *Sensor & Actuators* **B70** 87

Carney C M, Yoo S and Sheikh A A 2005 *Sensors & Actuators* **B108** 29

Chen Y J, Zhu C L and Xio G 2008 *Sensors & Actuators* **B129** 639

Coronado J M, Kataoka S, Tejedor T and Anderson M A 2003 *J. Catal.* **219** 219

Devi G S, Hyodo T, Shimizu Y and Egashira M 2002 *Sensors & Actuators* **B87** 122

Dhawale D S, Salunkhe R R, Patil U M, Gurav K V, More A M and Lokhande C D 2008 *Sensor & Actuators* **B134** 988

Faramarz H B, Kesmhiri M, Kakavand M and Troczynski T 2005 *Sensors & Actuators* **B110** 28

Guidi V, Carotta M C, Ferroni M, Martinelli G, Paglialonga L, Comini E and Sberveglieri G 1999 *Sensors & Actuators* **B57** 197

Kirner U, Schierbaum K D, Gopal W, Leibold B, Nicoloso N, Weppner W, Fischer D and Chu W F 1990 *Sensors & Actuators* **B1** 103

Kitamura T and Yokoyama M 1991 *J. Appl. Phys.* **69** 821

Lee K, Lee N H, Shin S H and Kim S J 2000 *Mater. Sci. Eng.* **B129** 109

Li M and Chen Y 1996 *Sensors & Actuators* **B32** 83

Liu Z, Yamazaki T, Shen Y, Kikuta T, Nakatani N and Li Y 2008 *Sensors & Actuators* **B129** 666

Manera M G, Cozzoli P D, Leo G, Curri M L, Agostiano A, Vasanelli L and Rella R 2007 *Sensors & Actuators* **B126** 562

Micheli A L 1984 *Am. Cer. Soc. Bull.* **63** 694

More A M, Gunjakar J L and Lokhande C D 2008 *Sensors & Actuators* **B129** 671

More P, Kumar R, Yadav B C and Khanna P K 2009 *Inter. J. Green Nanotechnol.: Mater. Sci. Eng.* **1** M3

Ruiz A M, Cornet A, Shimanoe K, Morante J R and Yamazoe N 2005 *Sensors & Actuators* **B108** 34

Shinde V R, Gujar T P and Lokhande C D 2007 *Sensors & Actuators* **B123** 701

Srivastava A, Jain K, Rashmi, Srivastava A K and Lakshmikumar S T 2006 *Mater. Chem. Phys.* **97** 85

Thiagarajan S, Su B W and Chen S M 2009 *Sensors & Actuators* **B136** 464

Wu Y 2009 *Sensors & Actuators* **B137** 80

Yadav B C, Srivastava A K and Sharma P 2007 *Sensor & Transducers* **181** 1348

Yadav B C, Srivastava R, Dwivedi C D and Pramanik P 2008a *Sensors & Actuators* **B131** 216

Yadav B C, Srivastava R, Yadav A and Srivastava V 2008b *Sensor Letts.* **6** 714

Yadav B C, Srivastava R and Yadav A 2009a *Sensors & Materials* **21** 87

Yadav B C, Yadav A, Shukla T and Singh S 2009b *Sensor Letts.* **7** 1